

An eccentrically perturbed Tonks-Girardeau gas

J. Goold

Centre for Quantum Technologies, National University of Singapore, Singapore,
Singapore

M. Krych, Z. Idziaszek

Faculty of Physics, University of Warsaw, 00-681 Warsaw, Poland

T. Fogarty, Th. Busch

Department of Physics, University College Cork, Cork, Ireland

Abstract. We investigate the static and dynamic properties of a Tonks-Girardeau gas in a harmonic trap with an eccentric δ -perturbation of variable strength. For this we first find the analytic eigensolution of the single particle problem and use this solution to calculate the spatial density and energy profiles of the many particle gas as a function of the strength and position of the perturbation. We find that the crystal nature of the Tonks state is reflected in both the lowest occupation number and momentum distribution of the gas. As a novel application of our model, we study the time evolution of the the spatial density after a sudden removal of the perturbation. The dynamics exhibits collapses and revivals of the original density distribution which occur in units of the trap frequency. This is reminiscent of the Talbot effect from classical optics.

1. Introduction

One of the standout achievements of ultracold atomic physics in the past decade has been the realisation of controllable and clean environments for the simulation of quantum manybody systems [1]. Cold atoms are ideal systems for such simulations and offer many desirable features, two of which are particularly unique. The first of these is the ability to tune the scattering length and hence the interaction in quantum gases. This is achieved by means of Feshbach resonances [2]. The second is the ability to change the dimensionality of the system and in particular to generate periodic geometries for atoms by means of optical lattice potentials [3]. Both of these separate developments, or their combination, allows experimentalists to enter regimes of strong correlation and explore complex condensed matter models. For instance, using optical lattice potentials the superfluid-Mott insulator phase transition has been observed by changing the lattice depth [3, 4]. In addition, by loading a BEC into a two-dimensional lattice and utilising strong confinement in the transverse direction, the achievement of lower dimensional systems was made possible and new quantum phases can now be explored with an incredible degree of precision. In the case of two dimensions, the famous Berezinskii-Kosterlitz-Thouless phase transition was observed recently [5] and for ultracold gases in one dimension one of the crowning achievements was the realisation of a unique model from many body theory [6] - the strongly correlated Tonks-Girardeau gas of hard core bosons [7, 8].

Since the first creation of a Tonks-Girardeau gas there have been further experimental studies focusing on the absences of thermalisation due to the integrability of the underlying Hamiltonian [9] and more recently on the density dynamics in the presence of an outcoupled impurity [10]. This second work has opened the door to studying the transport properties of impurities in ultracold quantum gases and therefore highlights the importance to understand the fundamental properties of a Tonks-Girardeau gas in the presence of an impurity. A number of studies in this direction already exist in the literature, in which the impurity is modelled using pseudo-potential approximation [11, 12, 13, 14, 15, 16]. These studies have primarily focused on fixed position perturbations and in this work we introduce a versatile analytical model which can be used to describe the Tonks-Girardeau gas in the presence of a perturbation of arbitrary strength at any position in a harmonic trap. In addition to describing a static impurity, this model can be interpreted as the limiting case of an split, asymmetric double well trap which may be realized using a sharply focused laser beam which is detuned from the atomic transition.

The paper is organised as follows: in Sec. 2 we briefly remind the reader of the Tonks-Girardeau gas and its solution by the Fermi-Bose mapping theorem. We then outline the eigensolution of a harmonically trapped single particle in the presence of an off-centre δ -perturbation in Sec. 3 and show in Sec. 4 how this can be used in combination with known techniques to characterise the groundstate of a many-particle gas. We then study the dynamics of the single particle density after a sudden removal of the perturbation as well as for a time-of-flight measurement. Finally, we conclude.

2. The Tonks-Girardeau gas

Optical lattices and atom chips allow to create trapping potentials that are tight enough in the transversal direction to freeze out all dynamics in these degrees of freedom [17]. A gas of N bosons in such a potential can then be approximated by the

one-dimensional Hamiltonian

$$\mathcal{H} = \sum_{n=1}^N \left[-\frac{\hbar^2}{2m} \frac{\partial^2}{\partial x_n^2} + V_{ext}(x_n) \right] + g_{1D} \sum_{i<j} \delta(|x_i - x_j|), \quad (1)$$

where m is the mass of the particles, V_{ext} is the trapping potential and g_{1D} is a 1D coupling constant which is derived from the renormalisation of the three-dimensional scattering process $g_{1D} = \frac{4\hbar^2 a_{3D}}{ma_{\perp}} (a_{\perp} - Ca_{3D})^{-1}$ [18]. Here a_{\perp} is the trap width and C is a constant of value 1.4603.... This Hamiltonian describes an inhomogeneous Lieb-Liniger gas, which in the strongly repulsive limit, $g_{1D} \rightarrow \infty$, can be solved by using a mapping to an ideal and spinless fermionic system [6]. This procedure is known as the Fermi-Bose mapping theorem and it can be used to show that the *local* density and correlation functions of this *strongly correlated* system are equivalent to the corresponding quantities of a *non-interacting* spin polarized Fermi gas. This strange equivalence is due solely to the dimensionality of the system - as the repulsive interactions become stronger, the particles are no longer free to overlap, thus mimicking the Pauli-exclusion principle in configuration space. The essential idea is that one can then treat the interaction term in eq. (1) by replacing it with a boundary condition on the allowed bosonic wave-function

$$\Psi_B(x_1, x_2, \dots, x_N) = 0 \quad \text{if} \quad |x_i - x_j| = 0, \quad (2)$$

for $i \neq j$ and $1 \leq i \leq j \leq N$. This is simply the hard core constraint which says that no probability exists for two particles ever to be at the same point in space. Such a constraint is automatically fulfilled by calculating the wave-function using a Slater determinant

$$\Psi_F(x_1, x_2, \dots, x_N) = \frac{1}{\sqrt{N!}} \det_{(n,j)=(0,1)}^{(N-1,N)} \psi_n(x_j), \quad (3)$$

where the ψ_n are the single particle eigenstates of the ideal system. This, however, leads to a fermionic rather than bosonic symmetry, which can be corrected by a multiplication with the appropriate unit antisymmetric function [6]

$$A = \prod_{1 \leq i < j \leq N} \text{sgn}(x_i - x_j), \quad (4)$$

to give $\Psi_B = A\Psi_F$. Knowing the single particle eigenstates is therefore a pre-requisite to being able to apply the mapping mechanism.

3. Single particle problem

The number of models in many particle quantum physics for which analytical solutions exist is extremely limited and often restricted to one spatial dimension [19]. Here we will describe one such model by studying the Hamiltonian (1) with

$$V_{ext}(x) = \frac{1}{2}m\omega^2 x^2 + \gamma\delta(x - d), \quad (5)$$

and $g_{1D} \rightarrow \infty$, which describes a Tonks-Girardeau gas in a harmonic trap of frequency ω which is split asymmetrically by a tunable δ -perturbation of strength γ a distance d from the centre of the trap. The limit $d = 0$ for this model is well known and has been studied extensively in recent years [11, 13, 14, 20]. In order to use the prescription of the mapping theorem one needs to first solve for the single particle eigenfunctions to build the Slater determinant (3). In this section we will study the eigensolution of

the single particle problem in detail. In fact, this problem is equivalent to the relative problem of two interacting atoms in separate harmonic traps which has recently been numerically solved in the three dimensional case [21]. We show below that this problem is analytical in one dimension.

The single particle Schrödinger equation for the potential (5) is given by

$$\left(\frac{-\hbar^2}{2m} \frac{d^2}{dx^2} + \frac{1}{2} m \omega^2 x^2 + \gamma \delta(x-d) \right) \psi_\nu(x) = \epsilon_\nu \psi_\nu(x), \quad (6)$$

where the energies are given by $\epsilon_\nu = (\nu + \frac{1}{2})\hbar\omega$. Let us rescale all of the units in terms of the undisturbed ($\gamma = 0$) trap length $l_0 = \sqrt{\frac{\hbar}{m\omega}}$ and energy $\hbar\omega$. In this way the equation (6) can be rewritten as

$$\left(\frac{d^2}{dx^2} + \nu + \frac{1}{2} - \frac{x^2}{2} - \kappa \delta(x-d) \right) \psi_\nu(x) = 0, \quad (7)$$

where $\kappa = \gamma l_0 / (\hbar\omega)$ is the re-normalised strength of the δ -barrier. On either side of the δ -function the solutions of the differential equation (7) are parabolic cylinder functions $D_\nu(x)$, which vanish for $x \rightarrow \infty$, but diverge for $x \rightarrow -\infty$. We can therefore write the solution piecewise as

$$\psi_\nu(x) = \psi_{l,\nu}(x)\theta(d-x) + \psi_{r,\nu}(x)\theta(x-d), \quad (8)$$

with

$$\psi_{r,\nu}(x) = N_+ D_\nu(x) \quad \text{and} \quad \psi_{l,\nu}(x) = N_- D_\nu(-x). \quad (9)$$

and $\theta(x)$ being the Heaviside function. The condition of continuity of these solutions at the position of the δ -function

$$N_+ D_\nu(-d) = N_- D_\nu(d), \quad (10)$$

together with the solution of the Schrödinger equation

$$-\int_{d-\epsilon}^{d+\epsilon} \psi_\nu''(x) dx + \int_{d-\epsilon}^{d+\epsilon} V(x) \psi_\nu(x) dx = \epsilon_\nu \int_{d-\epsilon}^{d+\epsilon} \psi_\nu(x) dx, \quad (11)$$

with

$$V(x) = \frac{1}{2} x^2 + \kappa \delta(x-d), \quad (12)$$

leads to a transcendental equation which determines the energy eigenvalues as a function of both, κ and d

$$N_+ D_\nu'(-d) + N_- D_\nu'(d) - 2\kappa N_+ D_\nu(-d) = 0. \quad (13)$$

The derivatives of the parabolic cylinder functions can be calculated using the recurrence relation [22]

$$D_\nu'(z) = \nu D_{\nu-1}(z) - \frac{1}{2} z D_\nu(z), \quad (14)$$

and for $D_\nu(d) \neq 0$ we find from eq. (10) the relation $N_- = N_+ D_\nu(-d) / D_\nu(d)$. Substituting these into eq. (13) we therefore find

$$\nu \left[D_{\nu-1}(-d) D_\nu(d) + D_{\nu-1}(d) D_\nu(-d) \right] = 2\kappa D_\nu(-d) D_\nu(d). \quad (15)$$

This equation determines the eigenenergies for the solutions that are nonzero at the position of the delta potential. To find the ones for which $D_\nu(d) = 0$ we can see from

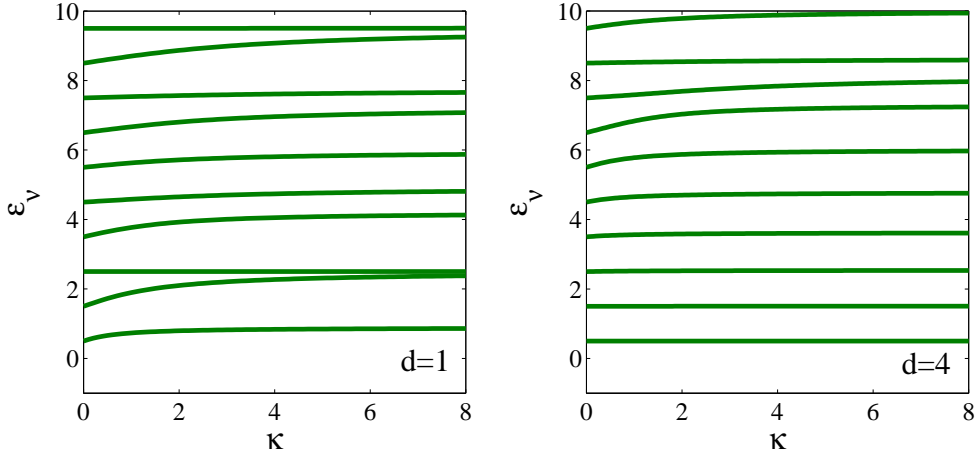


Figure 1. The energy spectrum of harmonically trapped particle in the presence of δ -like perturbation at position $d = 1$ and $d = 4$, for different strengths, κ , of the perturbation.

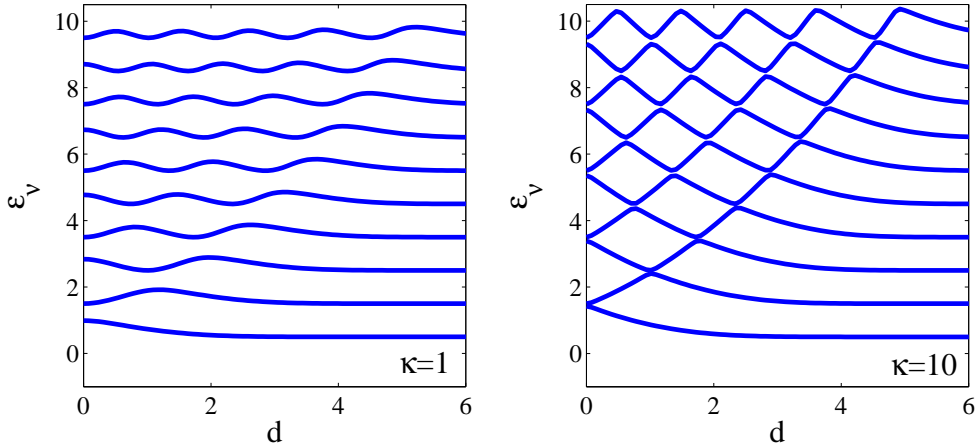


Figure 2. The energy spectrum of harmonically trapped particle in the presence of δ -like perturbation with strength $\kappa = 1$ and $\kappa = 10$, for various positions of the perturbation.

eq. (10) that $D_\nu(-d) = 0$, provided that $N_+ \neq 0$ and $N_- \neq 0$. Then eq. (13) reduces to

$$N_+ \nu D_{\nu-1}(-d) + N_- \nu D_{\nu-1}(d) = 0. \quad (16)$$

where the derivatives have been determined using eq. (14). The above equation together with the normalization of the total wave function determines N_+ and N_- for the solutions that vanish at the position of the delta potential. These solutions are independent of κ , and they correspond to the harmonic oscillator wave functions that vanish at $x = d$.

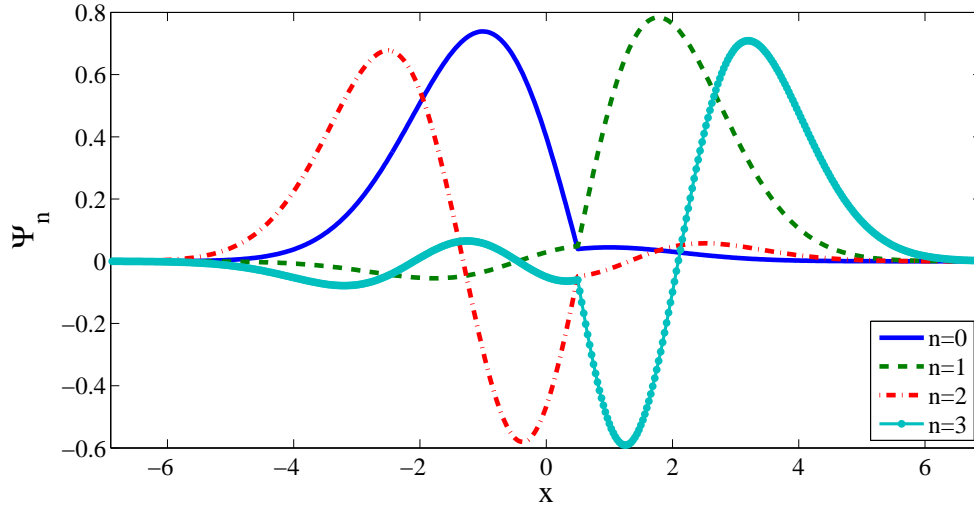


Figure 3. The lowest four eigenfunctions of a particle in a harmonic potential with a repulsive δ -function located at $d = 0.5$ of strength $\kappa = 10$

In Figs. 1 and 2 we show the energy spectrum as a function of d and κ , respectively. The presence of the perturbation introduces a non trivial structure in the spectrum and in general leads to an increase of the state's energy. The four lowest lying eigenfunction for $d = 0.5$ and $\kappa = 10$ are shown in Fig. 3. It can be seen that the presence of delta potential results in an abrupt change in the slope of the wavefunction at the position of the delta function and that the states are already highly localised on one side of the impurity for $\kappa = 10$.

4. Static and Dynamic Properties

4.1. Single Particle Density Profile

The single particle density is one of the most important observables for ultracold quantum gases. In the Tonks regime one can obtain it, even time-dependently, from the spectrum of underlying single particle Hamiltonian as [23]

$$\begin{aligned} \rho(x, t) &= N \int_{-\infty}^{+\infty} |\Psi_B(x, x_2, \dots, x_N; t)|^2 dx_2 \dots dx_N \\ &= \sum_{n=0}^{N-1} |\psi_n(x, t)|^2, \end{aligned} \quad (17)$$

where we have adopted the convention of labeling the first N eigenfunctions as $n = 0, 1, 2, \dots, N$.

In Fig. 4 we show this single particle density for a gas of 20 particles in a trap with an impurity of strength $\kappa = 10$ at three different positions in the trap. As expected the δ -impurity creates a significant local dip in the density and has only minimal effect at larger distances. The enhanced oscillations which are present around the position of the impurity are analogous to the famous Friedel oscillations which occur around an impurity in the surface charge density of a homogeneous electron gas [24].

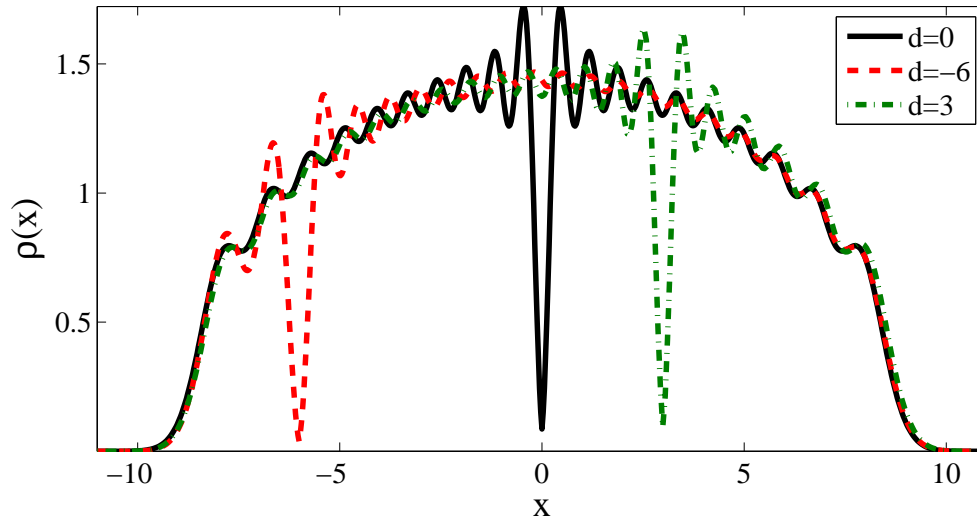


Figure 4. The single particle density of a harmonically trapped Tonks-Girardeau gas with 20 particles in equilibrium with a barrier of strength $\kappa = 10$, located at positions $d = 0, 3, -6$.

Let us in the following investigate the dynamical properties of such a gas by examining a non-equilibrium situation created by sudden removal of the impurity. In order to compute the time-dependent density of eq. (17) one needs to employ a time dependent basis. We obtain this basis numerically using the split operator method in the unperturbed harmonic trap. Alternatively one may simply employ the well known propagator for the harmonic oscillator to get the time dependent basis [25]. This can then be used to calculate the single particle density of eq. (17).

In Fig. 5 we show $\rho(x, t)$ following the sudden removal of an impurity of strength $\kappa = 10$ located at $d = -6$. One can see that the density dip formed by the impurity vanishes almost instantaneously, however a mirror image of the dip appears after half a trap period, $t = \pi/\omega$, and then again disappears followed by a complete revival after one trap period, $t = 2\pi/\omega$. This effect is analogous to the Talbot effect from classical optics where periodic refocusing of a diffraction grating is expected to occur in the near field of a transmitted wave. In this situation the δ -function represents the most trivial form of a diffraction grating. A natural question to ask is why is such an effect occurring in a strongly correlated *many* body system as the Talbot effect is a coherent *single* particle effect? The simple answer can be found by recalling that the system can be mapped onto free fermions, for which the single particle density is simply the sum of the squares of the single particle eigenfunctions, with each one undergoing its own coherent unitary evolution. In this picture, the occurrences can be explained by noting that all N eigenfunctions superimpose in phase again after every trap period and one finds that the density profile at odd multiples of π/ω is a mirror image of the initial density profile at $t = 0$. It is also worth noting that in between this revivals the density shows an interesting fine structure. This is shown in a close up of the density for the time period $0 \leq t \leq \pi$ in Fig. 6. When the impurity is removed, the matterwave readjusts to the profile of a harmonically trapped gas by a relaxation of

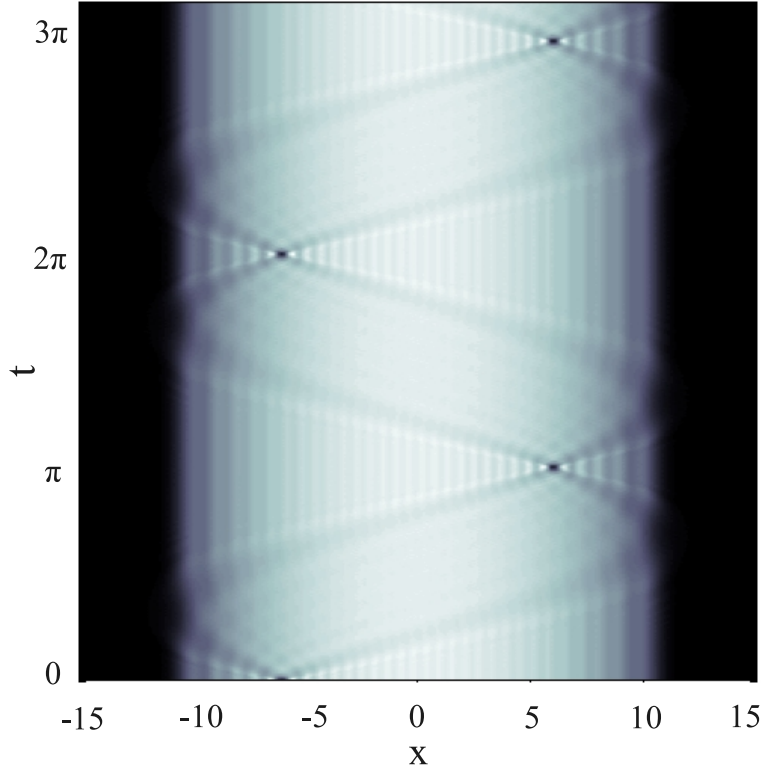


Figure 5. The time dependent single particle density of a harmonically trapped Tonks-Girardeau gas following the sudden removal of a δ barrier of strength $\kappa = 10$, located at position $d = -6$.

the Friedel oscillations. At $t = \pi/2$ there is complete relaxation of the oscillations, this is followed by a complete revival at $t = \pi$. This is precisely the fine structure we see in between revivals of the density dip in Fig. 5.

4.2. Energy profile

It is also interesting to consider the energy of the system as a function of the position of the impurity. Due to the Fermi-Bose duality, this can simply be calculated adding the eigenenergies of the single particle states up to the Fermi energy

$$E_{TG} = \sum_{n=0}^{N-1} \epsilon_n . \quad (18)$$

The energy profile for a gas of thirty particles for different δ -perturbation strengths as a function of the position of the perturbation is shown in Fig. 7. One can see a series of exactly fifteen lobes (the plot is symmetric for $d < 0$.), which become more pronounced as the strength of the perturbation is increased, but whose position is independent of this increase. The position of these local maxima correspond to the positions in which the probabilities for the single particle wavefunctions peak, highlighting the crystal structure of the ground state. The increase in energy due to the impurity is largest

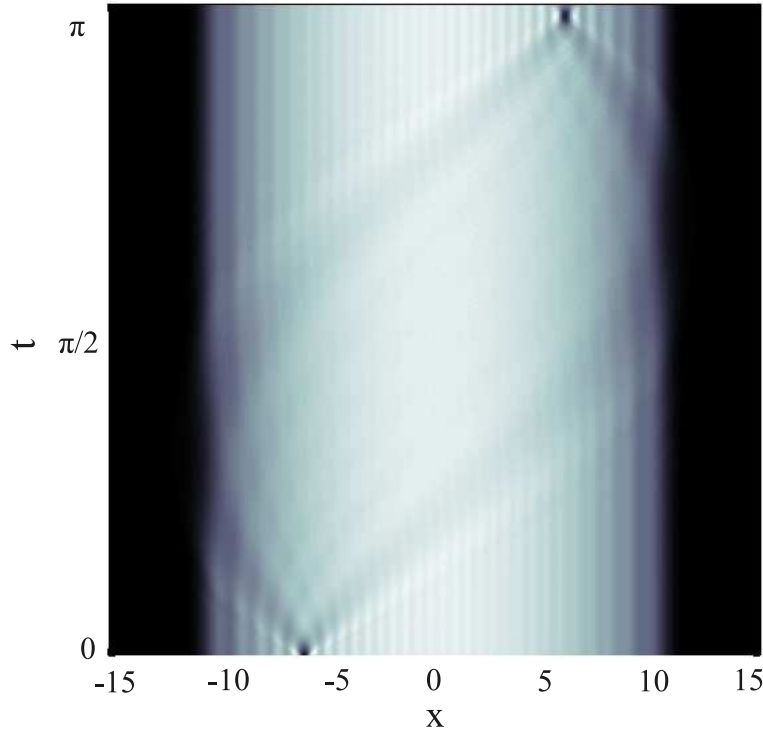


Figure 6. Detailed view of the time evolution of the single particle density for half a trap period.

when it is located at the centre of the cloud. In fact, one can view the perturbation as a probe which, when dragged adiabatically through a Tonks gas, makes it possible to gain information on the crystal structure of the state through an energy measurement. In the next section we will look at non-local properties of the ground state properties, which can be calculated from the reduced single particle density matrix.

4.3. Reduced single particle density matrix

The calculation of the reduced density matrix,

$$\rho^1(x, x', t) = N \int_{-\infty}^{\infty} \Psi_B^*(x, x_2, \dots, x_N, t) \times \Psi_B(x', x_2, \dots, x_N, t) dx_2 \dots dx_N, \quad (19)$$

and related observables for an ultracold gas is, in general, a difficult feat. The dimension of the integral in eq. (19) increases with particle number and this is very demanding on computer memory resources. For a Tonks gas in a harmonic potential, studies have therefore mainly used numerical methods such as Monte-Carlo integration to calculate the RSPDM [26], but some analytic work has also been done in this direction [27]. Recently, an exceptionally efficient algorithm for calculating the RSPDM of a Tonks-Girardeau gas in an arbitrary external potential has been presented by Pezer and Buljan [28]. This algorithm allows for a numerically exact

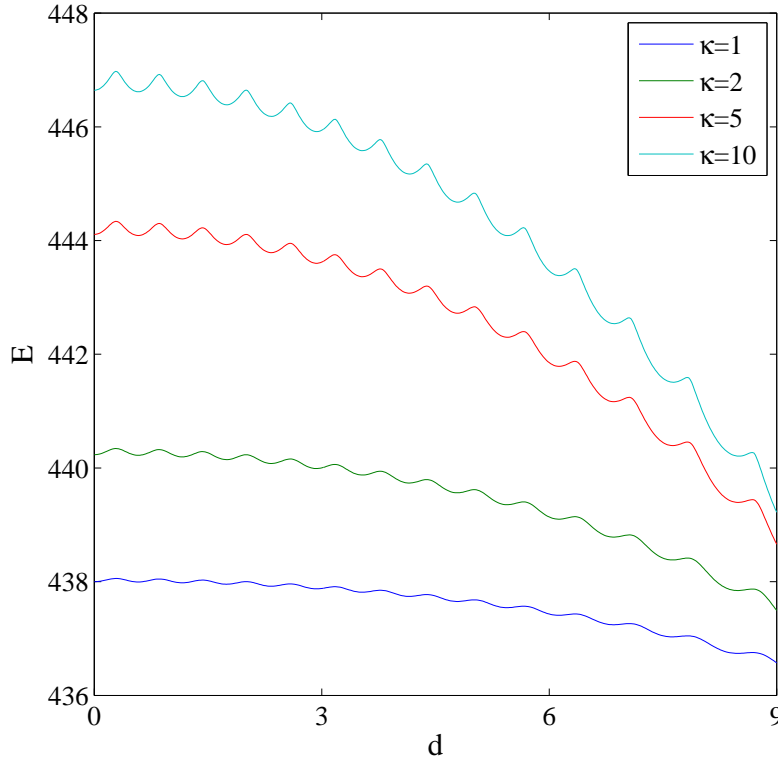


Figure 7. The energy of a harmonically trapped Tonks-Girardeau gas of $N=30$ particles as a function of the position of the δ -perturbation.

calculation of the RSPDM for a large number of particles with limited memory resources and at a rapid computational speed. The algorithm works for both time dependent and time independent potentials. The essential idea is that $\rho^1(x, x', t)$ can be expressed in terms of the dynamically evolving single particle energy eigenbasis, $\psi_i(x, t)$, as

$$\rho^1(x, x', t) = \sum_{i,j}^N \psi_i^*(x, t) A_{ij}(x, x', t) \psi_j(x', t). \quad (20)$$

The $N \times N$ matrix, $\mathbf{A}(x, x', t)$, is given by

$$\mathbf{A}(x, x', t) = (\mathbf{P}^{-1})^T \det \mathbf{P}, \quad (21)$$

where the entries of the matrix \mathbf{P} are computed as

$$P_{ij}(x, x', t) = \delta_{ij} - 2 \int_x^{x'} d\xi \psi_i^*(\xi, t) \psi_j(\xi, t), \quad (22)$$

and where δ_{ij} is the Kronecker delta. Given a pair of points (x, x') and the single particle basis functions $\psi_i(x, t)$ one can calculate the RSPDM of a Tonks gas by merely calculating an $N \times N$ matrix P , its inverse and its determinant, which is a significant saving on computational resources.

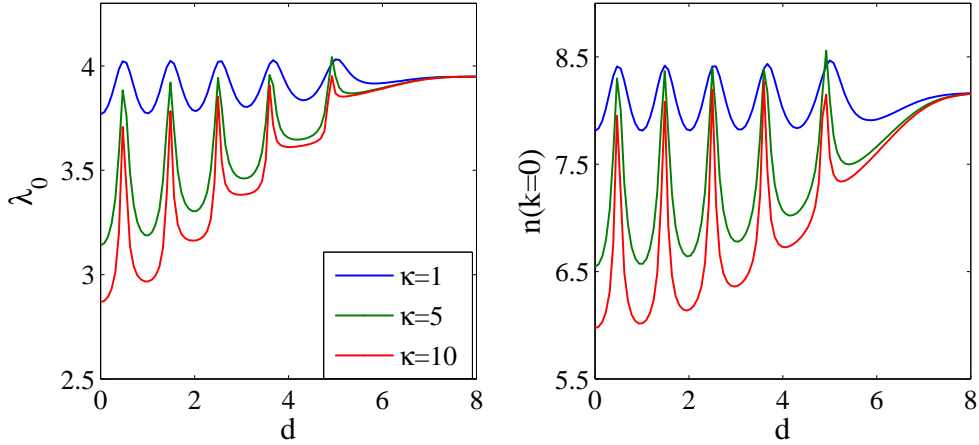


Figure 8. The largest eigenvalue of the RSPDM λ_0 and the peak of the momentum distribution $n(k=0)$ as a function of eccentricity d for perturbation strengths $\kappa = 1, 5, 10$ for a Tonks-Girardeau gas of $N = 10$ particles.

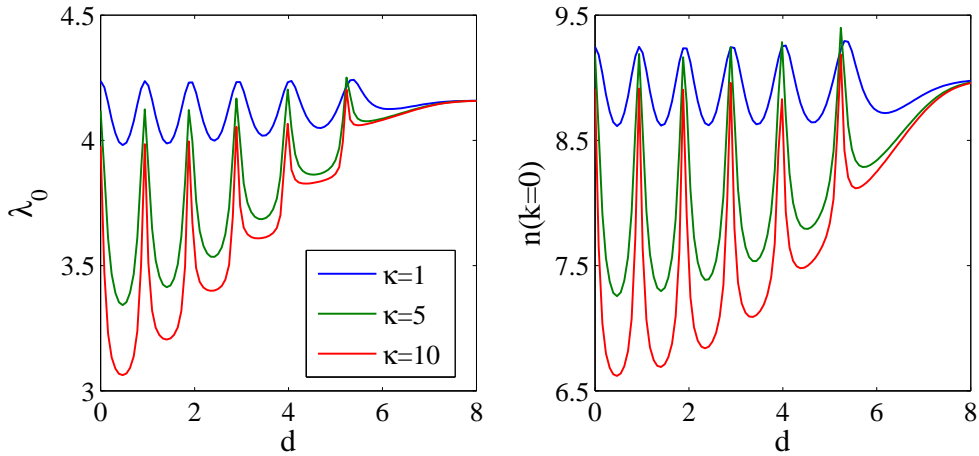


Figure 9. The largest eigenvalue of the RSPDM λ_0 and the peak of the momentum distribution $n(k=0)$ as a function of eccentricity d for perturbation strengths $\kappa = 1, 5, 10$ for a Tonks-Girardeau gas of $N = 11$ particles.

The RSPDM is a hermitian matrix and one can therefore write its spectral decomposition as

$$\rho^1(x, x', t) = \sum_{i=0} \lambda_i(t) \phi_i^*(x, t) \phi_i(x', t). \quad (23)$$

The eigenvectors, ϕ_i , are often referred to as natural orbitals in many-body physics and they provide an alternative basis of orthonormal single particle states for the many-body system. The eigenvalues, λ_i , are known as the occupation numbers obeying the normalisation condition $\sum_i \lambda_i = N$. The expansion in eq. (23) is extremely useful

for understanding the ground state properties of cold atomic gases, as the natural orbitals are defined not only for an ideal gas but also for interacting, thermal and non-uniform gases. In order to obtain the eigenvectors and eigenvalues of the reduced density matrix, one must solve the integral value equation,

$$\int dx' \rho^1(x, x', t) \phi_i(x', t) = \lambda_i(t) \phi_i(x, t). \quad (24)$$

The fraction of particles that are in the lowest lying orbital $\phi_0(x, t)$ is related to the largest eigenvalue λ_0 of the RSPDM by $f = \frac{\lambda_0}{N}$. Therefore, in analogy to the macroscopic occupation of a single eigenstate in a Bose-Einstein condensate, this orbital is sometimes referred to as the *BEC* state and the quantity λ_0 can act as a measure of the coherence in the system.

Another important measure of coherence can be derived from the momentum distribution of the gas which is defined as

$$n(k, t) = (2\pi\hbar)^{-1} \int \int \rho^1(x, x', t) e^{\frac{ik(x-x')}{\hbar}} dx dx' \quad (25)$$

$$= \sum_i \lambda_i(t) |\mu_i|^2, \quad (26)$$

where $\mu_i = (2\pi\hbar)^{-\frac{1}{2}} \int dx e^{\frac{ikx}{\hbar}} \phi_i(x, t)$ are the Fourier transforms of the natural orbitals. For a homogenous, non-interacting Bose gas at zero temperature the momentum function is a δ -function, reflecting the macroscopic occupation of the lowest natural orbital, whereas in the strongly interacting Tonks-Girardeau gas in equilibrium, the momentum distribution is comprised of a non-trivial distribution of quasi-momenta. The amplitude of the peak of the momentum distribution at $k = 0$ can therefore also be used to measure the spatial coherence present in the system. It is well known that this quantity does not follow a trivial behaviour in a disturbed, strongly interacting gas and that it in particular can show a dependence on having an even or an odd number of particles [13, 29, 30, 31]. In Fig. 8 we show both quantities defined above, λ_0 and $n(k = 0)$, as a function of distance of the perturbation from the trap centre for gas of $N = 10$ particles. As expected, both quantities exhibit similar features dominated by an oscillatory structure which becomes more pronounced as the strength of the δ -perturbation increases. As in the interpretation of the energy oscillations, the maxima correspond to positions where the single particle eigenstates have large probabilities, i.e. where the position of the δ -potential corresponds to a lattice point of the underlying crystal structure of the Tonks gas. For comparison in Fig. 9 we show the same quantities for the $N = 11$ case. In this case we see a maximum of coherence at $d = 0$, as symmetry reasons require a single particle to sit in the centre of the trap for odd particle numbers [13]. This dependence of the coherence on the position of the disturbance and can be experimentally observed by measuring the visibility in an interference experiment. We show in Fig. 10 the single particle density for a gas of $N = 10$ particles for which the disturbance is either located at a maximum of coherence (left panel), or at a minimum of the coherence (right panel). The difference in the visibility of the interference fringes is clearly observable.

5. Conclusions

In conclusion we have introduced a model to describe the harmonically trapped Tonks-Girardeau gas in the presence of a δ -perturbation of arbitrary strength and eccentricity.

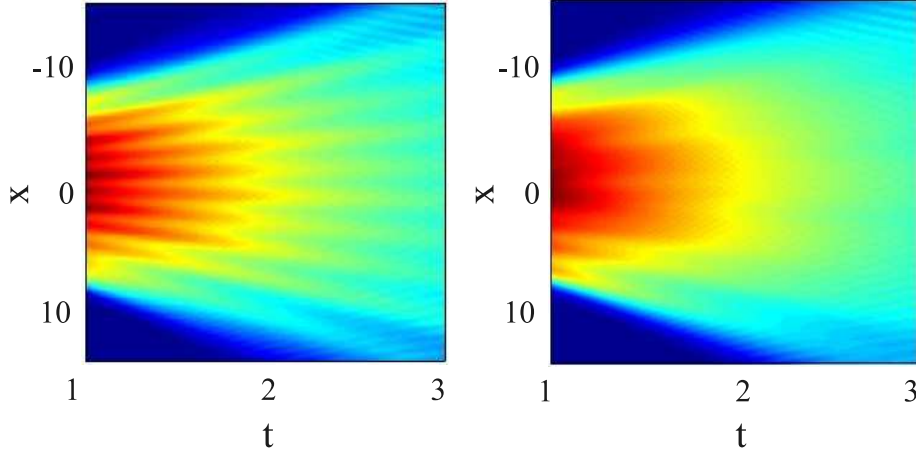


Figure 10. Single particle density of the free evolution of the gas after release from the trapping potential. Two cases are shown, (a) the delta barrier is positioned at $d = -0.5$ corresponding to a maximum coherence and (b) where the delta barrier is positioned at $d = -1$ corresponding to minimum coherence. Interference fringes indicate greater spatial coherence which confirms predictions of Fig.8.

We have clearly outlined the solution of the fundamental single particle problem and shown how it can be used in combination with known techniques to describe the groundstate properties of the gas. We have calculated the energy profile of the gas in the presence of the impurity and found an undulating profile as the perturbation is displaced through the gas, which highlights the crystal structure of the Tonks groundstate. In addition, we have calculated the momentum distribution and largest eigenvalue of the RSPDM as a function of both the eccentricity and strength of the perturbation. Again, we have found that these properties reflect the highly localised nature of the particles in the Tonks gas. Furthermore as a novel application of our model we have investigated the time density dynamics after a sudden removal of the perturbation. We find that the gas exhibits the classical Talbot effect with the image of the impurity reappearing at multiples of the inverse trap frequency. Given the recent experiments on out-of equilibrium dynamics of a Tonks gas [9, 10], it is an interesting extension of our work to study the dynamics of a moving impurity. This is currently work in progress.

6. Acknowledgements

This work was supported by the National Research Foundation and Ministry of Education, Singapore and Science Foundation Ireland under grant No. 05/IN/I852. JG would like to thank Elica Kyoseva for interesting discussions and MK would like to thank Agnieszka Witkowska for invaluable inspiration. TF acknowledges support from IRCSET under the Embark Initiative No.RS/2009/1082. ZI acknowledges financial support from Polish Government Research Grant for years 2007-2010. TB would like to thank Mauro Ferreira for helping to stimulate this work.

Bibliography

- [1] I. Bloch, J. Dalibard and W. Zwerger, *Rev. Mod. Phys.* **80**, 885 (2008).
- [2] Ph. Courteille, R.S. Freeland, D.J. Heinzen, F.A. van Abeelen and B.J. Verhaar, *Phys. Rev. Lett.* **81**, 69 (1998).
- [3] M. Greiner, O. Mandel, T. Esslinger, T.W. Hänsch and I. Bloch, *Nature* **415**, 39 (2002).
- [4] D. Jaksch, C. Bruder, J.I. Cirac, C. Gardiner and P. Zoller, *Phys. Rev. Lett.* **81**, 3108, (1998).
- [5] Z. Hadzibabic, P. Krüger, M. Cheneau, B. Battelier and J. Dalibard, *Nature* **441**, 1118 (2006).
- [6] M. Girardeau, *J. Math. Phys.* **1**, 516 (1960).
- [7] B. Paredes, A. Widera, V. Murg, O. Mandel, S. Fölling, I. Cirac, G.V. Shlyapnikov, T.W. Hänsch and I. Bloch, *Nature* **429**, 277 (2004).
- [8] T. Kinoshita, T. Wenger and D.S. Weiss, *Science* **305**, 1125 (2004).
- [9] T. Kinoshita, T. Wenger and D.S. Weiss, *Nature* **440**, 900 (2006).
- [10] S. Palzer, C. Zipkes, C. Sias and M. Köhl, *Phys. Rev. Lett.* **103**, 150601 (2009).
- [11] Th. Busch and G. Huyet, *J. Phys. B: At. Mol. Opt.* **36**, 2553 (2003).
- [12] H. Fu and A.G. Rojo, *Phys. Rev. A* **74**, 013620 (2006).
- [13] J. Goold and Th. Busch, *Phys. Rev. A* **77**, 063601 (2008).
- [14] J. Goold, D. O'Donoghue and Th. Busch, *J. Phys. B: At. Mol. Opt.* **41**, 215301 (2008).
- [15] M. Girardeau and A. Minguzzi, *Phys. Rev. A* **79**, 033610 (2009).
- [16] J. Goold, H. Doerk, Z. Idziaszek, T. Calarco and Th. Busch, *Phys. Rev. A* **81**, 041601 (2010).
- [17] H. Moritz, T. Stöferle, M. Köhl, and T. Esslinger, *Phys. Rev. Lett.* **91**, 250402 (2003).
- [18] M. Olshanii, *Phys. Rev. Lett.* **81**, 938 (1998).
- [19] B. Sutherland, *Beautiful Models*, (World Scientific Publishing Company, 2004).
- [20] D.S. Murphy, J.F. McCann, J. Goold and Th. Busch, *Phys. Rev. A* **76**, 053616 (2007).
- [21] M. Krych and Z. Idziaszek, *Phys. Rev. A* **80**, 022710 (2009).
- [22] M. Abramowitz and I. Stegun, eds., *Handbook of Mathematical Functions* (Dover, 1972).
- [23] M. Girardeau and E.M. Wright, *Phys. Rev. Lett.* **84**, 5239 (2000).
- [24] J. Friedel, *Nouvo Cimento* **7**, 287 (1958).
- [25] R.P. Feynman and A.R. Hibbs, *Quantum Mechanics and Path Integrals*, (McGraw-Hill, New York, 1965).
- [26] M.D. Girardeau, E.M. Wright, and J.M. Triscari, *Phys. Rev. A* **63**, 033601 (2001).
- [27] G.J. Lapeyre, Jr., M.D. Girardeau, and E.M. Wright, *Phys. Rev. A* **66**, 023606 (2002).
- [28] R. Pezer and H. Buljan, *Phys. Rev. Lett.* **98**, 240403 (2007).
- [29] X. Yin, Y. Hao, S. Chen, and Z. Zhang, *Phys. Rev. A* **78**, 013604 (2008).
- [30] K. Lelas, D. Jukić and H. Buljan, *Phys. Rev. A* **80**, 053617 (2009).
- [31] X. Lü, X. Yin and Y. Zhang, *Phys. Rev. A* **81**, 043607 (2010).

